RAPID REPORT | *Higher Neural Functions and Behavior*

Predicting an individual's dorsal attention network activity from functional connectivity fingerprints

 David E. Osher,[1] James A. Brissenden,[2] and David C. Somers[2]

[1]*Department of Psychology, The Ohio State University, Columbus, Ohio; and* [2]*Department of Psychological and Brain Sciences, Boston University, Boston, Massachusetts*

Osher DE, Brissenden JA, Somers DC. Predicting an individual's dorsal attention network activity from functional connectivity fingerprints. *J Neurophysiol* 122: 232–240, 2019. First published May 8, 2019; doi:10.1152/jn.00174.2019.—The cortical dorsal attention network (DAN) is a set of parietal and frontal regions that support a wide variety of attentionally demanding tasks. Whereas attentional deployment reliably drives DAN activity across subjects, there is a large degree of variation in the activation pattern in individual subjects. We hypothesize that a subject's own idiosyncratic pattern of cortical DAN activity can be predicted from that subject's own unique pattern of functional connectivity. By modeling task activation as a function of whole brain connectivity patterns, we are able to define the connectivity fingerprints for the frontal and parietal DAN, and use it to predict a subject's characteristic DAN activation pattern with high accuracy. These predictions outperform the standard group-average benchmark and predict a subject's own activation pattern above and beyond predictions from another subject's connectivity pattern. Thus an individual's distinctive connectivity pattern accounts for substantial variance in DAN functional responses. Last, we show that the set of connections that predict cortical DAN responses, the frontal and parietal DAN connectivity fingerprints, is predominantly composed of other coactive regions, including regions outside of the DAN including occipital and temporal visual cortices. These connectivity fingerprints represent defining computational characteristics of the DAN, delineating which voxels are or are not capable of exerting top-down attentional bias to other regions of the brain.

NEW & NOTEWORTHY The dorsal attention network (DAN) is a set of regions in frontoparietal cortex that reliably activate during attentional tasks. We designed computational models that predict the degree of an individual's DAN activation using their resting-state connectivity pattern alone. This uncovered the connectivity fingerprints of the DAN, which define it so well that we can predict how a voxel will respond to an attentional task given only its pattern of connectivity, with outstanding accuracy.

attention; connectivity fingerprint; functional connectivity; vision

---

INTRODUCTION

The cortical dorsal attention network (DAN) has been repeatedly defined across a multitude of PET and functional MRI (fMRI) studies spanning over two decades (Brissenden et al. 2016; Corbetta et al. 1993; Corbetta and Shulman 2002; Fox

et al. 2005; Gao and Lin 2012; Hagler and Sereno 2006; Kastner and Ungerleider 2001; Konen and Kastner 2008; Mackey et al. 2017; Power et al. 2011; Ptak and Schnider 2011; Scolari et al. 2015; Sheremata et al. 2010; Silver et al. 2005; Swisher et al. 2007; Szczepanski et al. 2010; Vossel et al. 2014; Yeo et al. 2011). Typical neuroimaging studies examining the DAN employ group analyses that reveal a robust set of regions in frontal and parietal cortices (Corbetta and Shulman 2002; Kastner and Ungerleider 2001; Scolari et al. 2015). These include the intraparietal sulcus and superior parietal lobule within the parietal lobe, as well as superior and inferior precentral sulcus within lateral frontal cortex (Corbetta and Shulman 2002; Fox et al. 2005; Gao and Lin 2012; Power et al. 2011; Ptak and Schnider 2011; Szczepanski et al. 2010; Yeo et al. 2011; see also Brissenden et al. 2016). Despite the reliability of these group-level regions, individual subjects are nonetheless variable in their specific anatomical pattern of DAN activity. Furthermore, the DANs of individual subjects have highly variable connectivity patterns (Braga and Buckner 2017; Gordon et al. 2017; Mueller et al. 2013). This led us to hypothesize that a subject's unique pattern of DAN activity might be explained, and therefore predicted, by that subject's pattern of intrinsic functional connectivity (Passingham et al. 2002).

To test how well DAN activation can be predicted by connectivity, we adopted a technique developed by Osher et al. (2016), Saygin et al. (2011), and Tavor et al. (2016), which attempts to identify a functional region's connectivity fingerprint (Mars et al. 2018; Passingham and Wise 2012), which is the connectivity pattern that specifically differentiates that functional brain region from other functional brain regions. An underlying assumption is that the functional specificity of a brain region depends largely on the pattern of connections it makes with other brain regions and therefore patterns of connectivity can be employed to reveal functional domains in individual brains.

Connectivity fingerprinting methods for predicting individual subject task activation have also been successfully implemented for a variety of brain regions and tasks (Cole et al. 2016; Parker Jones et al. 2016; Saygin et al. 2016; Smittenaar et al. 2017; Tavor et al. 2016; Wang et al. 2017). This technique attempts to elucidate the defining connectivity pattern (the connectivity fingerprint) for a brain region for a particular task, by directly modeling blood oxygen level-dependent (BOLD)

---

responses as a function of whole brain connectivity patterns at the level of an individual data point (here, surface vertices) within an anatomically restricted search space of each individual subject. In this study, we examine functional connectivity between cortical surface vertices within a search space of interest (i.e., posterior parietal cortex, lateral frontal cortex) and cortical parcellations outside the search space. Specifically, the resulting fingerprint model for each search space is a vector describing the connectivity of the subset of vertices within the search space that share a common functional response of interest to all parcels outside the search space. By modeling the relationship between resting-state correlations and task responses, we can both *1*) isolate the frontal and parietal DAN connectivity fingerprints, the principal cortical connections underlying cortical DAN activation, among the complex pattern of connectivity across the brain and *2*) use the connectivity fingerprint to predict DAN activation profiles of subjects from connectivity alone, as opposed to relying on group-averaging techniques that can obscure individual subject differences.

We demonstrate that the DAN connectivity fingerprint model is able to very accurately predict an individual's pattern of activation within frontal and parietal cortex. These predictions are more accurate than a group-average benchmark model and are selective to a subject's own connectivity pattern. Finally, we show that the frontal and parietal cortical DAN connectivity fingerprints relate strongly to activation in other areas: connectivity to regions that are highly predictive of DAN activity tend to be highly coactive themselves.

MATERIALS AND METHODS

Subjects. Nine healthy subjects participated in this study (3 women). All subjects were right-handed and had normal or corrected-to-normal vision. Subjects ranged in age from 24 to 38 yr. The Institutional Review Board of Boston University approved the study. All subjects were compensated, gave written informed consent to participate in the study, and were screened for MRI contraindications before scanning commenced. Subjects were recruited from Boston University and the Greater Boston area.

Visual stimuli and experimental paradigm. Stimuli were generated using the Psychophysics Toolbox (Brainard 1997; Pelli 1997) in MATLAB (The MathWorks, Natick, MA) and displayed using an LCD projector onto a screen inside the scanner bore. Subjects fixated on a centrally located crosshair while 12 oriented colored bars were presented (6 in each hemifield). Whereas the number of presented bars in each hemifield was held constant across trials, the number of items to be remembered that were presented within a given block was either 0, 1, or 4. The remaining bars in the display served as distractors. The zero target condition served as a sensorimotor control condition. Target and distractors were distinguished by color, with targets shown in red and distractors shown in blue. Target and distractor colors remained fixed over the experiments so as to not add a cognitive switching component to the task. Each bar subtended $0.25° \times 2.5°$ of visual angle. Targets were limited to either the right or left hemifield (counterbalanced across blocks). All bars in the display were randomly oriented at one of four possible angles ($0°$, $45°$, $90°$, $135°$). Each subject completed eight runs (total time per run = 6 min, 16 s). Each fMRI task run contained ten 34-s task blocks (4 blocks of attend 4 targets, 4 blocks of attend 1 target, and 2 blocks of sensorimotor control, with 2 block orders that alternated across runs) and 16 s of blank fixation before and after the task blocks. Each block of trials consisted of a 2-s cue indicating the location of the target stimuli (left or right hemifield), followed by eight 4-s trials. On each trial, a memory sample display was presented for 200 ms. Subjects were instructed to maintain the orientations of the presented target items

over a 1,000-ms delay period. After the sample and delay period, a memory probe was presented for 1,800 ms. A 1,000-ms fixation period separated each trial. On 50% of trials, one of the target bars changed its orientation from the sample period to the probe period, whereas on the other 50% of trials, no changed occurred. Subjects could respond during either the memory probe or the intertrial fixation period by pressing a key to indicate that the orientation of the target had changed or a separate key if it had not changed. The magnitude of the change on change trials was held constant at $90°$ (e.g., $0° \rightarrow 90°$ or $45° \rightarrow 135°$). During sensorimotor control blocks, subjects were presented a display consisting entirely of distractors (all blue) and were instructed to press either key during the probe or intertrial fixation period. The response button box was operated by the index and middle fingers of the subject's right hand. Subjects also underwent two to three resting-state scans with identical scan parameters (each 180 TRs; 6-min duration). Resting-state scans were obtained in either the same scan session (8/9 subjects) or a different session. During the resting-state scans, subjects were instructed to let their minds wander while maintaining fixation on a centrally located crosshair.

Magnetic resonance image acquisition. Data were acquired from a 3-Tesla Siemens TIM Trio magnetic resonance imager located at the Center for Brain Science at Harvard University (Cambridge, MA). A 32-channel head coil was used for all scans. A high-resolution ($1.0 \times 1.0 \times 1.3$ mm) magnetization-prepared rapid gradient-echo sampling structure scan was acquired for each subject. The cortical surface of each hemisphere was then computationally reconstructed from this anatomical volume using FreeSurfer software (version 5.3.0; https://surfer.nmr.mgh.harvard.edu/; Dale et al. 1999; Fischl 2012). T2*-weighted echo-planar imaging (EPI) BOLD images were acquired using a slice-accelerated EPI sequence that permits simultaneous multislice acquisitions using the blipped-controlled aliasing in parallel imaging technique (TR = 2 s, TE = 30 ms, flip angle = $80°$, 6/8 partial Fourier acquisition; Setsompop et al. 2012). A total of 69 slices were acquired with a slice acceleration factor of 3 and 0% skip, covering the whole brain. Images were acquired at a nominal 2-mm isotropic spatial resolution (matrix size = $108 \times 108 \times 69$).

fMRI data preprocessing. Functional data were preprocessed using the FreeSurfer FS-FAST software package. Data were first slice-time corrected and motion corrected. Following analysis with FS-FAST, images were surface-registered to "fsaverage" (MNI305) template space. *T*-statistic maps from the contrast of attend 4 targets > sensorimotor control were used for predictions, because the activation pattern from this contrast is more robust than that produced by the contrasts of attend 4 > attend 1 and attend 1 > sensorimotor control. Resting-state data were additionally spatially smoothed (3-mm full-width half-maximum). Resting-state data were then further preprocessed in MATLAB using custom scripts. We performed nuisance signal regression of head motion (6 motion parameters and their 6 temporal derivatives), whole brain signal, and ventricular and white matter signals (Van Dijk et al. 2010). We then calculated framewise displacement by taking the sum of the absolute derivatives of the six motion parameters for each time point (Power et al. 2012). A threshold of 0.5 mm was set to identify time points with excessive motion. To avoid artifact spread during bandpass filtering, high-motion time points were replaced using linear interpolation (Carp 2013). Bandpass filtering was then performed (0.01–0.08 Hz). After filtering, high-motion time points were removed.

Search spaces and target regions, and functional connectivity. Search spaces and target regions were created from the multimodal parcellation (MMP) of Glasser et al. (2016) in fsaverage, which is composed of 180 regions in each hemisphere. Frontal and parietal search spaces were defined by combining all regions that contain the DAN in every subject, using the contrast of attend 4 targets > sensorimotor control using a liberal threshold of $P < 0.05$, to generate a large enough search space that would include each subject's DAN with high certainty. The frontal search space contained the following regions from the MMP, for both hemi-

spheres: 6a, 6ma, 6d, 6v, 6r, i6–8, 8Av, 8C, 55b, FEF, PEF, IFJp, IFJa, and IFSp. The parietal search space contained the following regions from the MMP, for both hemispheres: V7, IP0, IP1, IPS1, IP2, AIP, LIPd, LIPv, VIP, MIP, 7PL, 7PC, 7AL, and PFt.

Functional connectivity was calculated as the Pearson correlation coefficient between the resting-state time course of each vertex of a search space and the mean resting-state time course across all vertices of each target parcel. Target regions were defined as all other MMP regions not included in the search space. This analysis yielded a $v \times p$ matrix of correlations (a functional connectome) for each subject hemisphere, for both the frontal and parietal models, where v is the number of vertices in the search space and p is the number of target parcels.

DAN predictions. Connectivity fingerprint (CF) models were constructed using a leave-one-subject-out approach to permit cross-validation using the subject's actual task data. Therefore, nine CF models, each leaving out a different subject, were constructed for each hemispheric search space (parietal, frontal). A CF model was a vector of length p, the number of target parcels. CF model predictions of a subject's task activation within the model search space were a vector of length v, the number of vertices in the search space. Predictions were generated by computing the dot product between the individual's functional connectome (i.e., vertex-to-parcel connectivity matrix) and the CF model coefficients, which was constructed without any data from that subject.

CF models were constructed from functional connectivity and task data using ridge regression (Hastie et al. 2009), also known as Tikhonov regularization. The ridge regression model was built using standardized data (mean centered and SD set to 1) with connectivity values as the design matrix and *t*-statistic values (attend > sensorimotor control) as responses; individual data points were single vertices in the frontal or parietal search space, concatenated across subjects. The model was trained using a nested leave-one-subject-out routine, which is an iterative approach wherein all of the data of the subject whose DAN is to be predicted is kept aside and not used for modeling whatsoever; this is the "outer loop" of cross-validation. With the remaining data, nested "inner loops" of similar cross validation are then iteratively performed, to predict the DAN of each remaining subject. Each inner loop is performed 100 times, each time using a different regularization coefficient (the lambda parameter) from a set of values logarithmically spaced between 10^{-5} and 10^2. The optimal lambda was chosen from the set of inner loop models that minimized the average mean squared prediction errors across subjects ($\mathrm{argmin}\frac{1}{n}\sum MSE_k$ for k lambdas in n subjects). The mean model coefficients across inner loops for the selected lambda were then computed, and the resulting vector was multiplied by the connectivity matrix of the outer loop left-out subject, to produce the final predicted DAN responses for that subject. Thus the model and parameter selection is completely independent of the left-out subject. To reiterate this procedure from the bottom up, in each inner loop, connectivity and BOLD responses from all vertices of a search space of all $N - 2$ subjects are modeled by ridge regression with 100 different regularization parameters; the coefficients from the best-fitting model are retained, and these coefficients from each inner loop are then averaged across all $N - 2$ subjects and then applied to the outer, left-out subject's connectivity data, to generate predictions for that subject. This procedure is then repeated for all subjects. The model coefficients for the connectivity fingerprints (i.e., see Fig. 4A) were produced in exactly the same way, except that a single loop of hyperparameter-optimizing cross-validations was used, to generate a single model. Prediction accuracy was assessed as the correlation between the predicted and observed values for an individual subject (Tavor et al. 2016).

Group-average benchmark. The group-average benchmark was produced using a leave-one-subject-out procedure. For each left-out subject, a random effects general linear model was fit (using Free-Surfer) to the contrast estimates of all other subjects. This was performed on the fsaverage template surface. Thus the group-average benchmark was slightly different for each subject, because their own data were excluded from the analysis. Prediction accuracy was assessed as described above, using the correlation between the predicted values from the group average and the observed values for each subject.

Predictions from other subjects' connectivity. We compared the accuracy of predictions generated from a subject's own connectivity pattern with predictions generated from other subjects' connectivity. After training the CF model for each left-out subject and for each search space, we applied the model to the connectivity pattern of each other subject (by multiplying the vector of model coefficients with the connectivity matrix for each subject), resulting in nine predicted activity patterns for each subject (1 for themselves, using the model built by leaving them out, and 8 built from the models that left out each other subject). These were then compared with the left-out subject's actual activation pattern. We then tested the difference between prediction accuracy from subjects' own connectivity against predictions from other subjects' connectivity, using two-sample *t*-tests.

RESULTS

We aimed to elucidate the connectivity fingerprint of the parietal and frontal portions of the DAN using intrinsic functional connectivity and task-based BOLD activity. We designed computational models to learn the relationship between connectivity and task-based DAN activity; the resulting models, i.e., the DAN connectivity fingerprints, were then applied to independent subjects' connectivity data to predict those subjects' unique task activation. We evaluated the predictions by comparing them to the actual DAN activity pattern for each individual.

To elicit DAN activation, we employed a change detection visual working memory task (Fig. 1*A*), which has been shown to robustly recruit putative DAN frontoparietal areas (Huettel et al. 2001; Sheremata et al. 2010; Todd and Marois 2004; Xu and Chun 2006). Frontal and parietal search spaces were defined from the multimodal parcellation of Glasser et al. (2016), by combining all parcels that unequivocally contained the DAN in all subjects (Fig. 1*B*; see MATERIALS AND METHODS). All other regions from this parcellation were used as targets (346 targets for the frontal search space and 346 for the parietal search spaces). For each subject hemisphere, we aimed to predict the pattern of task activation for each vertex within each search space. To construct our models, we extracted, for each vertex within each search space, the degree of activation during the task (attend > sensorimotor control), as well as its resting-state correlation with each target region. We modeled task activation as a function of the whole brain pattern of connectivity using ridge regression under a nested leave-one-subject-out cross-validation routine (Fig. 1*C*; see MATERIALS AND METHODS).

Predictions for frontal DAN. The resulting predictions were remarkably accurate: the mean Pearson's correlation between subjects' actual responses and predicted responses was 0.65 ± 0.052 for the left hemisphere (LH) frontal DAN and 0.67 ± 0.077 for the right hemisphere (RH). These predictions were so accurate that we felt it appropriate to showcase the results of every subject (Fig. 2). Note that the unique pattern of each subject's DAN activation was faithfully captured by connectivity-based predictions. For example, the right hemisphere of *subject 1* has four frontal loci that are strongly activated, and
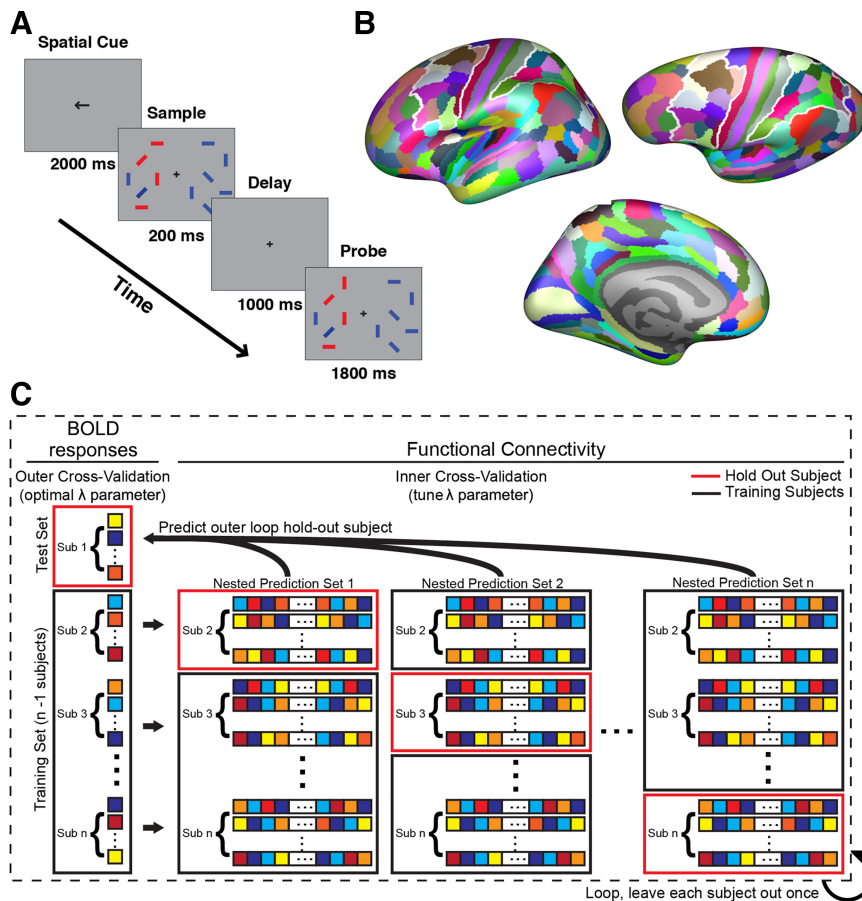
Fig. 1. Task and methods schematic. *A*: blood oxygen level-dependent (BOLD) data were acquired while subjects performed a change detection task. Participants were instructed to attend to the orientation of the red target items and to ignore irrelevant distractors (blue). After a short delay, participants indicated whether any of the attended items had changed orientation from the sample to the probe display. *B*: the multimodal parcellation from Glasser et al. (2016) was used to define targets and search spaces. The frontal and parietal search spaces are outlined in white. All parcels not part of a search space were included as targets. *C*: dorsal attention network activation and functional connectivity were modeled with a nested leave-one-subject-out cross validation routine, using ridge regression. All vertices were iteratively held out for a single subject, and the lambda hyperparameter (λ; regularization coefficient) of the ridge was optimized within an additional loop of cross-validation across the remaining subjects. The coefficients from the optimal inner-loop models were averaged and then used to generate predictions for the outer-loop subject using only that subject's connectivity pattern. Sub, subject.

the subject's whole brain connectivity pattern accurately predicts each of these loci. As a benchmark comparison, we also generated group-average maps, using a leave-one-subject-out approach (see MATERIALS AND METHODS). Building a functional atlas based on group averaging of task data is a standard technique for identifying functional areas in individual subjects. In the present study, this approach is fairly accurate across subjects (mean LH correlation with actual was 0.46 ± 0.033; mean RH correlation was 0.39 ± 0.059). The group average captures what is common across subjects spatially, but fails at finding unique features of individual subjects' activation patterns; by contrast, the connectivity model captures what is common across subjects' connectivity fingerprint for DAN activation, which in turn more accurately matches their individual functional response profiles. The connectivity-based predictions significantly outperformed the group-average benchmark in both hemispheres [LH: $P = 5.8 \times 10^{-4}$, $t_{(8)} = 5.5$; RH: $P = 2.1 \times 10^{-4}$, $t_{(8)} = 6.4$].

Predictions for parietal DAN. The parietal search space yielded even greater accuracy than the frontal search space: the mean correlation between subjects' actual responses and predicted responses was 0.73 ± 0.053 in the LH and 0.73 ± 0.069 in the RH (Fig. 2). The group average also yielded very good predictions in the parietal search space. For the LH, the mean correlation was 0.45 ± 0.036, and for the RH, the mean correlation was 0.54 ± 0.037. However, the connectivity-based predictions significantly outperformed the group-average benchmark once again [LH: $P = 3.8 \times 10^{-4}$, $t_{(8)} = 5.8$; RH: $P = 3.0 \times 10^{-3}$, $t_{(8)} = 4.2$].

Specificity of a subject's own connectivity pattern and DAN response. Next, we assessed how strongly a subject's own connectivity pattern relates to his or her specific DAN response profile (see MATERIALS AND METHODS). We compared each subject's DAN responses with predictions built from each other subject's connectivity patterns to ask, "Does a subject's unique connectivity pattern predict their own, idiosyncratic DAN, above and beyond the connectivity of a different subject?" We found this to be significantly true in all subjects in both frontal and parietal search spaces, and in both hemispheres, with only one exception (Fig. 3, Table 1). Across the group, in the frontal search space, subjects' own connectivity patterns significantly predict their DAN responses better than other subjects' connectivity in both hemispheres (LH: mean within subjects = 0.65 ± 0.052, mean other subjects = 0.29 ± 0.015; RH: mean within subjects = 0.67 ± 0.077, mean other subjects = 0.27 ± 0.019, $P < 0.0001$). The same was true for the parietal search space (LH: mean within subjects = 0.73 ± 0.053, mean other subjects = 0.36 ± 0.018; RH: mean within subjects = 0.73 ± 0.069; mean other subjects = 0.43 ± 0.018, $P < 0.0001$). Thus individual differences in DAN activation are explained best by an individual's own connectivity, rather than the general connectivity pattern of a region.

Connectivity fingerprints. The model coefficients (Fig. 4) describe the connectivity pattern that is best associated with DAN activation, representing its connectivity fingerprints. In other words, if a vertex is strongly connected to the positive predictors (e.g., anterior insula) and weakly connected to negative predictors (e.g., temporal parietal junction), then it is likely that
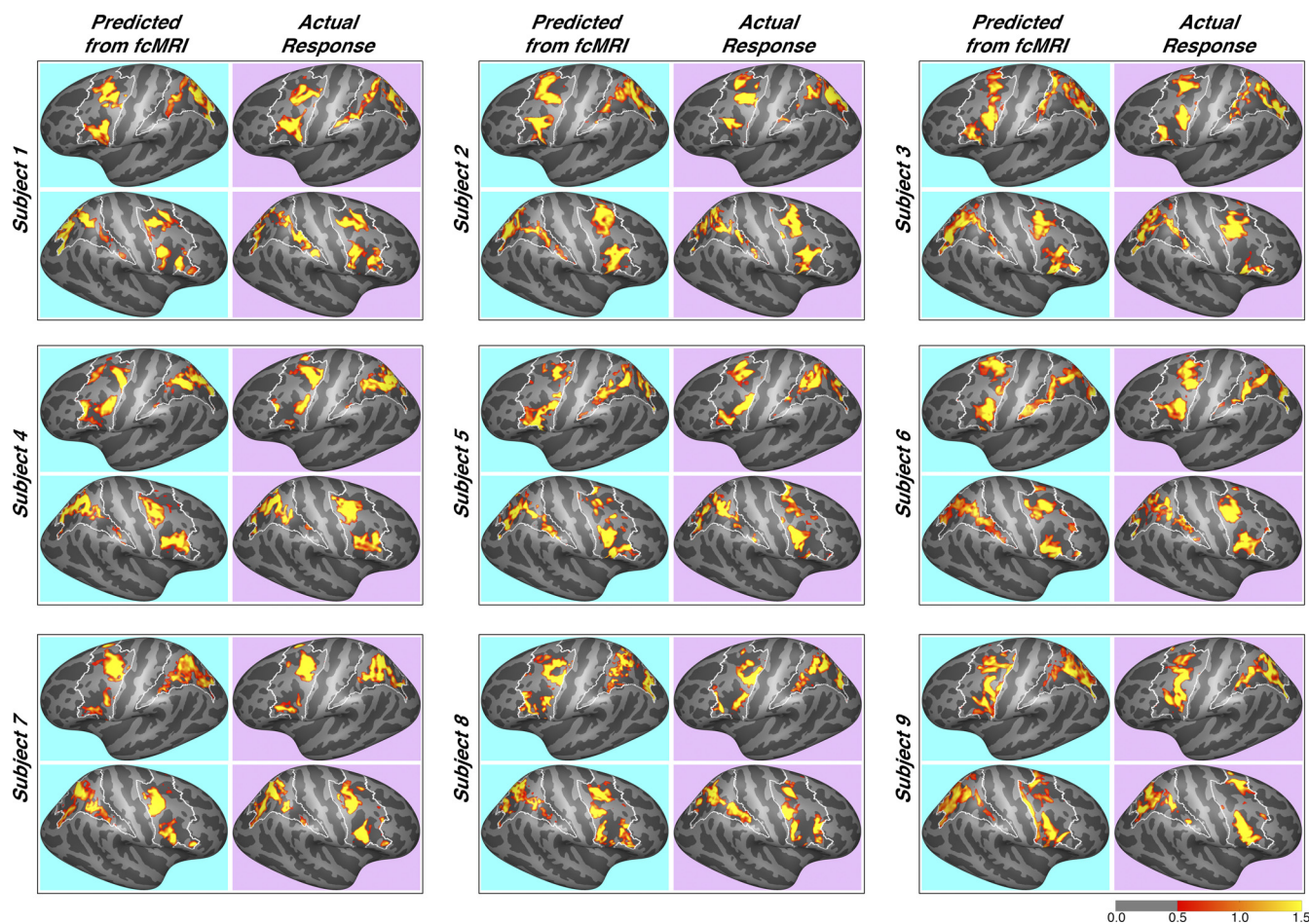
Fig. 2. Predicted dorsal attention network (DAN) activation for each subject. Predictions for all 9 subjects are shown, juxtaposed with their actual observed responses, for both frontal and parietal search spaces. Color scale is in Z scores. Note the variation in DAN activation profiles across individual subjects, which is accurately accounted for by the connectivity-based predictions. fcMRI, functional connectivity magnetic resonance imaging.

this vertex is part of the DAN. Interestingly, there is a striking relationship between the DAN connectivity fingerprints and the whole brain activation pattern to an attentionally demanding task. The Pearson correlation between the parcelwise mean responses and the frontal DAN coefficients was $r = 0.62$ in the LH and $r = 0.64$ in the RH. For the parietal DAN, this relationship was also significant in both hemispheres: $r = 0.71$ in the LH and $r = 0.64$ in the RH (all $P < 0.0001$). Thus the more responsive a parcel is, the more predictive its connectivity pattern. It is important to note that the modeling procedure does not include any information about the responses of connected regions and in no way ensures that responsive regions would be especially predictive. Nonetheless, the connectivity fingerprints for the frontal and parietal DAN exhibit a robust pattern wherein the regions that are recruited by an attentionally demanding task are also highly predictive of DAN responses. This includes the intraparietal sulcus and superior parietal lobule for the frontal DAN, and superior and inferior regions in the precentral sulcus for the parietal DAN. Both search spaces are predicted by low- and high-level visual areas in occipital and temporal cortices, as well as regions in the cognitive control network, including anterior insular cortex and anterior cingulate cortex (for the frontal DAN only). Regions with negative model coefficients are less connected to more responsive DAN vertices

and include the temporal parietal junction, posterior cingulate cortex, and ventral medial prefrontal cortex (especially for the parietal DAN). Interestingly, the frontal and parietal search spaces diverged in their connectivity fingerprints in the anterior cingulate and ventral medial prefrontal cortex, which were negative for the parietal search space and positive for the frontal search space.

DISCUSSION

We show here that connectivity fingerprint modeling of cortical DAN activity produces highly accurate predictions at the smallest measurable unit of data, single cortical surface vertices, across individual subjects. These findings demonstrate how strongly connectivity can characterize activity in the frontal and parietal portions of the DAN and how an individual subject's spatial variability of DAN activation aligns precisely with a multivariate map of whole brain connectivity. Moreover, we show that connectivity-based predictions are more accurate than independent group-average predictions, which are a standard method for predicting an individual's functional response map from other subjects' data. A group-average map represents what is consistent across subjects spatially, rather than what is unique about an individual subject's DAN. Whole brain connectivity, on the other hand, can shift spatially from subject to subject and is
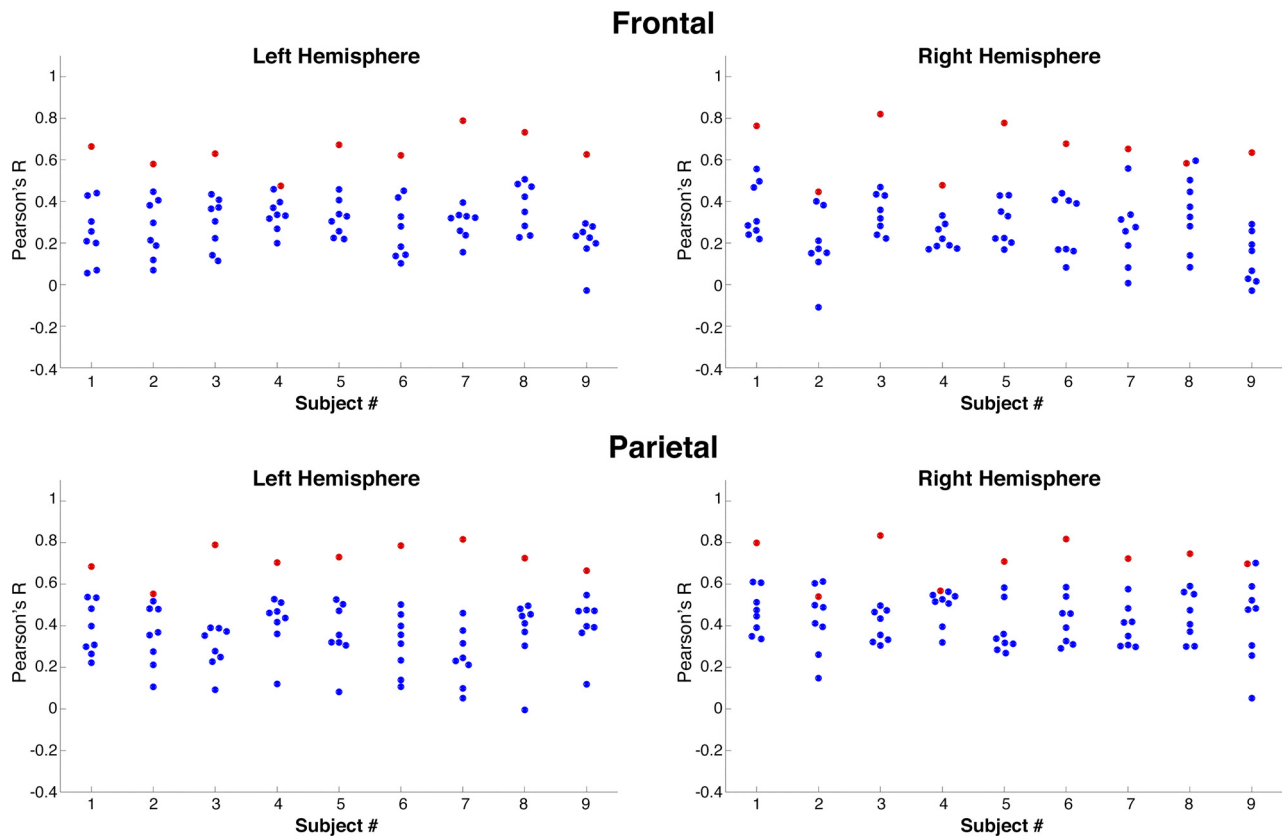
Frontal

Parietal

Fig. 3. Prediction accuracy depends on subjects' unique connectivity pattern. For each subject and for each region of interest, predictions were generated from a subject's own connectivity (red) or from each other subject's connectivity (blue). In all but one case, a subject's unique pattern of dorsal attention network responses is best predicted from his or her own connectivity (right hemisphere parietal region of *subject 2*).

unconstrained by location information alone; our results show that the spatially impartial connectivity data is superior at predicting task activity within the DAN compared with the spatial information alone of the group average.

Table 1. *Prediction accuracy from a subject's own connectivity vs. predictions from other subjects' connectivity*

	Left Hemisphere		Right Hemisphere	
	Corrected P value	$t_{(7)}$ statistic	Corrected P value	$t_{(7)}$ statistic
Frontal subject				
1	4.20×10^{-5}	9.87	1.71×10^{-5}	11.30
2	2.03×10^{-4}	7.18	2.07×10^{-3}	4.86
3	5.62×10^{-5}	9.18	1.25×10^{-6}	21.02
4	1.18×10^{-3}	5.25	1.14×10^{-5}	12.42
5	5.98×10^{-6}	14.25	1.87×10^{-6}	17.93
6	6.00×10^{-5}	8.88	4.42×10^{-5}	9.53
7	2.18×10^{-7}	27.04	1.54×10^{-4}	7.67
8	1.98×10^{-5}	11.43	4.31×10^{-3}	4.15
9	5.98×10^{-6}	14.31	5.41×10^{-6}	14.46
Parietal subject				
1	1.07×10^{-4}	8.12	2.17×10^{-5}	11.71
2	3.64×10^{-3}	4.28	9.68×10^{-2}	1.92
3	2.21×10^{-6}	19.35	5.36×10^{-7}	23.75
4	1.07×10^{-4}	8.24	3.25×10^{-2}	2.74
5	7.20×10^{-5}	9.40	5.75×10^{-5}	9.25
6	1.21×10^{-5}	12.85	8.34×10^{-6}	14.40
7	2.73×10^{-6}	16.96	2.17×10^{-5}	11.28
8	1.07×10^{-4}	8.27	5.75×10^{-5}	9.15
9	2.42×10^{-4}	6.98	4.77×10^{-3}	4.27

P values are corrected using the Benjamini-Hochberg method.

The present findings add to a growing body of work demonstrating the efficacy of connectivity fingerprinting methods for predicting individual subject task activation. Connectivity fingerprinting was initially developed using structural connectivity data (Osher et al. 2016; Saygin et al. 2011, 2016; Smittenaar et al. 2017; Wang et al. 2017) and has been expanded to employ functional connectivity (Parker Jones et al. 2016; Tavor et al. 2016) as employed in the present study. Prior work successfully implemented CF models for a variety of brain regions and tasks, including the Human Connectome Project data set (Tavor et al. 2016), reward signals in striatum (Smittenaar et al. 2017), language maps in presurgical patients (Parker Jones et al. 2016), selectivity in blind and sighted parahippocampal gyrus (Wang et al. 2017), development of the visual wordform area (Saygin et al. 2016), and extended as "activity flow" by weighting connectivity patterns with regional functional responses (Cole et al. 2016). In the present study, this approach successfully predicts frontal and parietal lobe activation during an attentionally demanding visual working memory task. These results also advance the possibility that there exist strong connectivity fingerprints for other aspects of visual cognition. Unlike analysis approaches that parcel the brain solely on the basis of resting-state data (e.g., independent components analysis), the connectivity fingerprinting approach constructs a model that directly predicts task-specific activation. It would be very interesting to examine differences within the DAN for different types of attention tasks, including working memory load manipulations, and assess how the connectivity fingerprints differ across varying
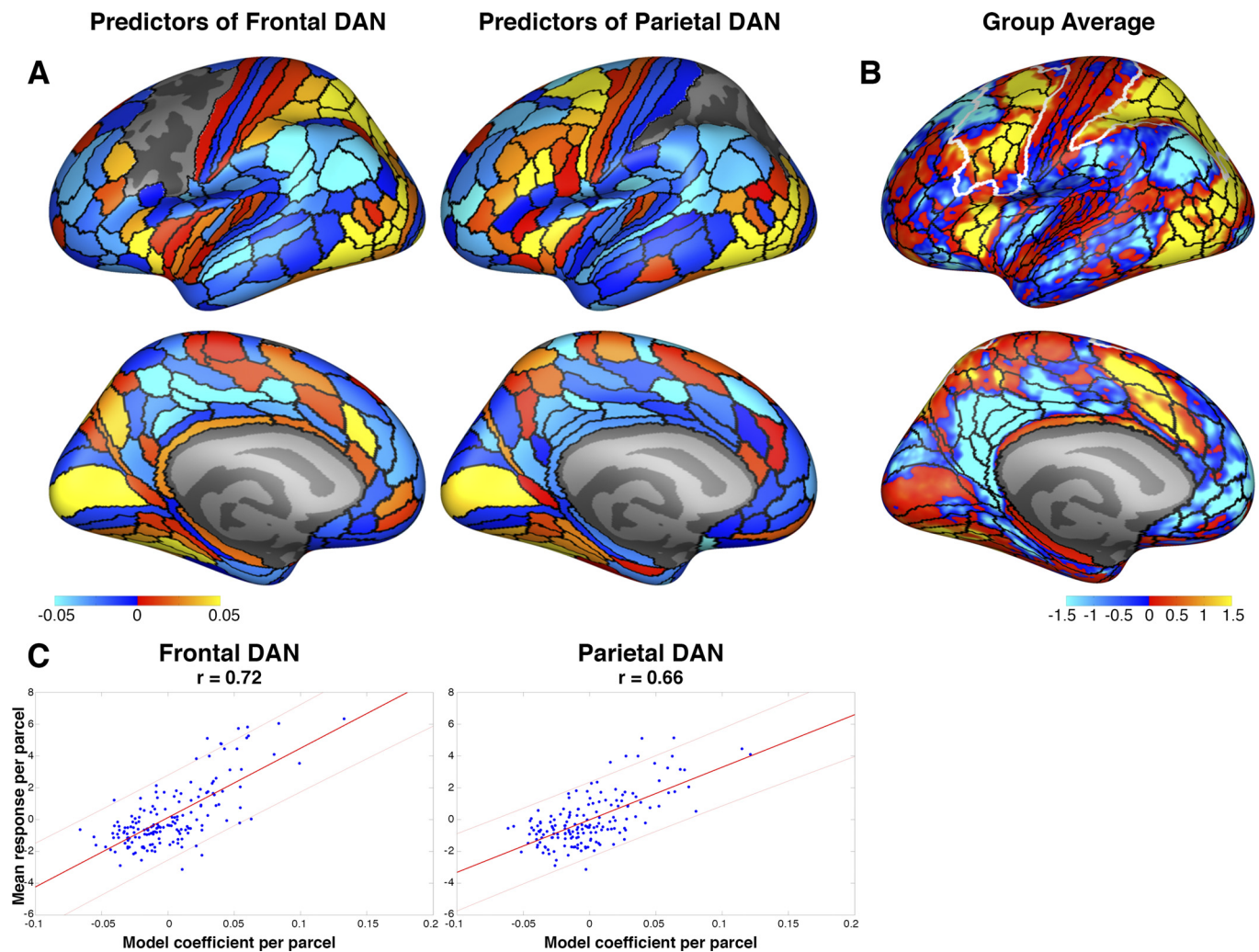
Fig. 4. Connectivity fingerprints for the dorsal attention network (DAN). *A*: the connectivity fingerprints for frontal and parietal DANs are shown at *left* and *right*, respectively, with the lateral view at *top* and medial view at *bottom*. Because the connectivity fingerprints of both hemispheres were extremely similar, they are averaged for visualization purposes. Hot colors depict regions whose connectivity predicts higher DAN activation, whereas cool colors depict regions whose connectivity predicts lower DAN activation. The empty regions on the lateral surfaces are the frontal and parietal search spaces where DAN activation was predicted (within-search spaces were excluded as targets). Color scale for these model coefficients is in arbitrary units. *B*: unthresholded group-average map with regional boundaries overlaid in black and search spaces in white. Color scale is in Z scores, as in Fig. 2. *C*: the DAN connectivity fingerprints strongly correlate with blood oxygen level-dependent (BOLD) responses. The model coefficients and mean BOLD responses of each parcel outside of the search spaces are plotted for the frontal (*left*) and parietal (*right*) DANs. Thick red lines denote best linear fit, and thin lines are 95% confidence intervals. Note that the responses of these regions are completely independent of the model itself, but nonetheless, the most responsive regions are the best predictors.

tasks and parameters, as well as how well each task predicts each other. Future studies could also use this technique to study the ventral attention network, which is recruited during sensory reorienting (Corbetta and Shulman 2002). The cognitive control network includes several regions that tend to be coactive with the DAN during attentionally demanding tasks (Cole et al. 2014; Cole and Schneider 2007), and in the present study were observed to contribute heavily to the connectivity fingerprint of the DAN. It would be enlightening to also investigate the connectivity fingerprint of the cognitive control network during tasks that selectively recruit it. The cerebellum has been increasingly noted for its involvement in guiding visual attention (Brissenden et al. 2016, 2018) and could be another interesting target for a connectivity fingerprinting analysis.

In the present study, the ability of DAN connectivity fingerprints to distinguish a subject's nuanced pattern of activation is best demonstrated by the observation that a subject's unique DAN activation pattern is best predicted by his or her own connectivity profile. The dramatic drop in accuracy when the connectivity of one subject is used to predict another's DAN implies that there exists a defining relationship between the functional responses and connectivity of an individual. Together with the group-average results, this suggests that spatial anatomical information obtained from group data does not account for an individual's DAN response pattern nearly as well as his or her own, unique pattern of connectivity, and that across subjects, whole brain connectivity patterns covary spatially with DAN responses.

In this study, robust predictions were obtained using large parietal and frontal search spaces. Each of those regions is known to contain multiple functional cortical areas, which may differ in their pattern of functional connectivity (e.g., Badre et

al. 2009; Hagler and Sereno 2006; Konen and Kastner 2008; Mackey et al. 2017; Michalka et al. 2015; Silver et al. 2005; Swisher et al. 2007). This suggests that the use of more restrictive search spaces could yield even more accurate predictions; nonetheless, the models find connectivity patterns that are common among voxels that respond similarly throughout the entire search space (even if they are spatially disparate).

Analysis of the resulting DAN connectivity fingerprint reveals a strong relationship to activation in other areas outside of the cortical DAN. Regions whose connectivity is highly predictive of DAN activity tend to be highly coactive themselves. This result makes sense but is remarkable because the only task-evoked data that were included in the model originated from the frontal or parietal search spaces; no information about the responses of other regions was included, and thus this phenomenon is not an artifactual product of the modeling procedure. Indeed, any other result could have been observed with equal likelihood, including the opposite, where the least responsive regions were predictive of DAN responses, or no relationship at all. Nonetheless, the connectivity fingerprint for the cortical DAN attentional response is primarily composed of strongly responsive regions; regions outside of the DAN that respond to an attention task are especially connected to the most responsive vertices within the DAN. Similar results were reported with face selectivity in the fusiform gyrus, whose connectivity fingerprint was composed of other components of the face network (Saygin et al. 2011), and across the brain for multiple visual categories, where the most selective regions were reported to constitute major hub nodes of brainwide connectivity fingerprints (Osher et al. 2016). Additionally, the regions where higher connectivity predicts lower DAN responses include many components of the default mode network (Greicius et al. 2003; Power et al. 2010, 2011; Raichle et al. 2001). This supports a corpus of literature that report robust anticorrelations between these networks (Fox et al. 2005, 2009; Power et al. 2011); the connectivity fingerprinting approach differs from this literature by directly modeling connectivity with neural responses, at the fine spatial grain of single voxels in individual subjects, and thus it delineates the connections that covary with the degree of DAN activation [as opposed to a region of interest (ROI)-based approach that treats each voxel equally within an ROI].

Finally, these findings offer several practical implications for research in cognitive and clinical neuroscience. First, the DAN is a burgeoning research interest, currently yielding hundreds of hits on PubMed. It is therefore of great interest to a large research community that we can now predict cortical DAN at the level of an individual subject with remarkably high accuracy. In the present experiment, subjects underwent over 50 min of task MRI, but between 12 and 18 min of resting-state MRI. Given that the cost of an hour of MRI scan time can often exceed $500, the potential to reduce scan time per subject and thus the scanning budget offers another possible benefit for a cognitive neuroscience laboratory. Furthermore, mounting evidence from several independent laboratories has shown that connectivity fingerprints can predict a variety of neural response patterns, including visual perception, visual and auditory attention, working memory, motor action, social cognition, reward, and language (Osher et al. 2016; Parker Jones et al. 2016; Saygin et al. 2011; Smittenaar et al. 2017; Tavor et al. 2016; Tobyne et al. 2018). A second implication for these

findings is that they enable otherwise inaccessible research into the DAN of subject pools that cannot perform fMRI experiments, such as those with low-functioning autism (Pardini et al. 2009). Third, these findings could be used for presurgical planning (see Parker Jones et al. 2016); surgeons can now use a cheaper and faster resting-state scan to identify with high confidence the location of the DAN, to avoid brain damage that might result in spatial neglect syndrome, even if the patient is currently unresponsive. Finally, predicting the DAN from a short resting-state scan will be powerful for exploring its development from very young ages (e.g., Saygin et al. 2016).

DISCLOSURES

No conflicts of interest, financial or otherwise, are declared by the authors.

AUTHOR CONTRIBUTIONS

D.E.O., J.A.B., and D.C.S. conceived and designed research; D.E.O. and J.A.B. performed experiments; D.E.O. analyzed data; D.E.O. and D.C.S. interpreted results of experiments; D.E.O. prepared figures; D.E.O. drafted manuscript; D.E.O., J.A.B., and D.C.S. edited and revised manuscript; D.E.O., J.A.B., and D.C.S. approved final version of manuscript.

REFERENCES

Badre D, Hoffman J, Cooney JW, D'Esposito M. Hierarchical cognitive control deficits following damage to the human frontal lobe. *Nat Neurosci* 12: 515–522, 2009. doi:10.1038/nn.2277.

Braga RM, Buckner RL. Parallel interdigitated distributed networks within the individual estimated by intrinsic functional connectivity. *Neuron* 95: 457–471.e5, 2017. doi:10.1016/j.neuron.2017.06.038.

Brainard DH. The Psychophysics Toolbox. *Spat Vis* 10: 433–436, 1997. doi:10.1163/156856897X00357.

Brissenden JA, Levin EJ, Osher DE, Halko MA, Somers DC. Functional evidence for a cerebellar node of the dorsal attention network. *J Neurosci* 36: 6083–6096, 2016. doi:10.1523/JNEUROSCI.0344-16.2016.

Brissenden JA, Tobyne SM, Osher DE, Levin EJ, Halko MA, Somers DC. Topographic cortico-cerebellar networks revealed by visual attention and working memory. *Curr Biol* 28: 3364–3372.e5, 2018. doi:10.1016/j.cub.2018.08.059.

Carp J. Optimizing the order of operations for movement scrubbing: comment on Power et al. *Neuroimage* 76: 436–438, 2013. doi:10.1016/j.neuroimage.2011.12.061.

Cole MW, Bassett DS, Power JD, Braver TS, Petersen SE. Intrinsic and task-evoked network architectures of the human brain. *Neuron* 83: 238–251, 2014. doi:10.1016/j.neuron.2014.05.014.

Cole MW, Ito T, Bassett DS, Schultz DH. Activity flow over resting-state networks shapes cognitive task activations. *Nat Neurosci* 19: 1718–1726, 2016. doi:10.1038/nn.4406.

Cole MW, Schneider W. The cognitive control network: integrated cortical regions with dissociable functions. *Neuroimage* 37: 343–360, 2007. doi:10.1016/j.neuroimage.2007.03.071.

Corbetta M, Miezin FM, Shulman GL, Petersen SE. A PET study of visuospatial attention. *J Neurosci* 13: 1202–1226, 1993. doi:10.1523/JNEUROSCI.13-03-01202.1993.

Corbetta M, Shulman GL. Control of goal-directed and stimulus-driven attention in the brain. *Nat Rev Neurosci* 3: 201–215, 2002. doi:10.1038/nrn755.

Dale AM, Fischl B, Sereno MI. Cortical surface-based analysis. I. Segmentation and surface reconstruction. *Neuroimage* 9: 179–194, 1999. doi:10.1006/nimg.1998. 0395.

Fischl B. FreeSurfer. *Neuroimage* 62: 774–781, 2012. doi:10.1016/j.neuroimage. 2012.01.021.

Fox MD, Snyder AZ, Vincent JL, Corbetta M, Van Essen DC, Raichle ME. The human brain is intrinsically organized into dynamic, anticorrelated functional networks. *Proc Natl Acad Sci USA* 102: 9673–9678, 2005. doi:10.1073/pnas.0504136102.

Fox MD, Zhang D, Snyder AZ, Raichle ME. The global signal and observed anticorrelated resting state brain networks. *J Neurophysiol* 101: 3270–3283, 2009. doi:10.1152/jn.90777.2008.

Gao W, Lin W. Frontal parietal control network regulates the anti-correlated default and dorsal attention networks. *Hum Brain Mapp* 33: 192–202, 2012. doi:10.1002/hbm.21204.

Glasser MF, Coalson TS, Robinson EC, Hacker CD, Harwell J, Yacoub E, Ugurbil K, Andersson J, Beckmann CF, Jenkinson M, Smith SM, Van Essen DC. A multi-modal parcellation of human cerebral cortex. *Nature* 536: 171–178, 2016. doi:10.1038/nature18933.

Gordon EM, Laumann TO, Adeyemo B, Petersen SE. Individual variability of the system-level organization of the human brain. *Cereb Cortex* 27: 386–399, 2017.

Greicius MD, Krasnow B, Reiss AL, Menon V. Functional connectivity in the resting brain: a network analysis of the default mode hypothesis. *Proc Natl Acad Sci USA* 100: 253–258, 2003. doi:10.1073/pnas.0135058100.

Hagler DJ Jr, Sereno MI. Spatial maps in frontal and prefrontal cortex. *Neuroimage* 29: 567–577, 2006. doi:10.1016/j.neuroimage.2005.08.058.

Hastie T, Tibshirani R, Friedman J. *The Elements of Statistical Learning: Data Mining, Inference, and Prediction* (2nd ed.). New York: Springer, 2009. doi:10.1007/978-0-387-84858-7.

Huettel SA, Güzeldere G, McCarthy G. Dissociating the neural mechanisms of visual attention in change detection using functional MRI. *J Cogn Neurosci* 13: 1006–1018, 2001. doi:10.1162/089892901753165908.

Kastner S, Ungerleider LG. The neural basis of biased competition in human visual cortex. *Neuropsychologia* 39: 1263–1276, 2001. doi:10.1016/S0028-3932(01)00116-6.

Konen CS, Kastner S. Two hierarchically organized neural systems for object information in human visual cortex. *Nat Neurosci* 11: 224–231, 2008. doi:10.1038/nn2036.

Mackey WE, Winawer J, Curtis CE. Visual field map clusters in human frontoparietal cortex. *eLife* 6: e22974, 2017. doi:10.7554/eLife.22974.

Mars RB, Passingham RE, Jbabdi S. Connectivity fingerprints: from areal descriptions to abstract spaces. *Trends Cogn Sci* 22: 1026–1037, 2018. doi:10.1016/j.tics.2018.08.009.

Michalka SW, Kong L, Rosen ML, Shinn-Cunningham BG, Somers DC. Short-term memory for space and time flexibly recruit complementary sensory-biased frontal lobe attention networks. *Neuron* 87: 882–892, 2015. doi:10.1016/j.neuron.2015.07.028.

Mueller S, Wang D, Fox MD, Yeo BT, Sepulcre J, Sabuncu MR, Shafee R, Lu J, Liu H. Individual variability in functional connectivity architecture of the human brain. *Neuron* 77: 586–595, 2013. doi:10.1016/j.neuron.2012.12.028.

Osher DE, Saxe RR, Koldewyn K, Gabrieli JD, Kanwisher N, Saygin ZM. Structural connectivity fingerprints predict cortical selectivity for multiple visual categories across cortex. *Cereb Cortex* 26: 1668–1683, 2016. doi:10.1093/cercor/bhu303.

Pardini M, Garaci FG, Bonzano L, Roccatagliata L, Palmieri MG, Pompili E, Coniglione F, Krueger F, Ludovici A, Floris R, Benassi F, Emberti Gialloreti L. White matter reduced streamline coherence in young men with autism and mental retardation. *Eur J Neurol* 16: 1185–1190, 2009. doi:10.1111/j.1468-1331.2009.02699.x.

Parker Jones O, Voets NL, Adcock JE, Stacey R, Jbabdi S. Resting connectivity predicts task activation in pre-surgical populations. *Neuroimage Clin* 13: 378–385, 2016. doi:10.1016/j.nicl.2016.12.028.

Passingham RE, Stephan KE, Kötter R. The anatomical basis of functional localization in the cortex. *Nat Rev Neurosci* 3: 606–616, 2002. doi:10.1038/nrn893.

Passingham RE, Wise SP. Ventral prefrontal cortex: generating goals based on visual and auditory contexts. In: *The Neurobiology of the Prefrontal Cortex: Anatomy, Evolution, and the Origin of Insight.* Oxford, UK: Oxford University Press, 2012, p. 195–219. doi:10.1093/acprof:osobl/9780199552917.003.0007.

Pelli DG. The VideoToolbox software for visual psychophysics: transforming numbers into movies. *Spat Vis* 10: 437–442, 1997. doi:10.1163/156856897X00366.

Power JD, Cohen AL, Nelson SM, Wig GS, Barnes KA, Church JA, Vogel AC, Laumann TO, Miezin FM, Schlaggar BL, Petersen SE. Functional network organization of the human brain. *Neuron* 72: 665–678, 2011. doi:10.1016/j.neuron.2011.09.006.

Power JD, Fair DA, Schlaggar BL, Petersen SE. The development of human functional brain networks. *Neuron* 67: 735–748, 2010. doi:10.1016/j.neuron.2010.08.017.

Power JD, Barnes KA, Snyder AZ, Schlaggar BL, Petersen SE. Spurious but systematic correlations in functional connectivity MRI networks arise from subject motion. *Neuroimage* 59: 2142–2154, 2012. doi:10.1016/j.neuroimage.2011.10.018.

Ptak R, Schnider A. The attention network of the human brain: relating structural damage associated with spatial neglect to functional imaging correlates of spatial attention. *Neuropsychologia* 49: 3063–3070, 2011. doi:10.1016/j.neuropsychologia.2011.07.008.

Raichle ME, MacLeod AM, Snyder AZ, Powers WJ, Gusnard DA, Shulman GL. A default mode of brain function. *Proc Natl Acad Sci USA* 98: 676–682, 2001. doi:10.1073/pnas.98.2.676.

Saygin ZM, Osher DE, Koldewyn K, Reynolds G, Gabrieli JD, Saxe RR. Anatomical connectivity patterns predict face selectivity in the fusiform gyrus. *Nat Neurosci* 15: 321–327, 2011. doi:10.1038/nn.3001.

Saygin ZM, Osher DE, Norton ES, Youssoufian DA, Beach SD, Feather J, Gaab N, Gabrieli JD, Kanwisher N. Connectivity precedes function in the development of the visual word form area. *Nat Neurosci* 19: 1250–1255, 2016. doi:10.1038/nn.4354.

Scolari M, Seidl-Rathkopf KN, Kastner S. Functions of the human fronto-parietal attention network: evidence from neuroimaging. *Curr Opin Behav Sci* 1: 32–39, 2015. doi:10.1016/j.cobeha.2014.08.003.

Setsompop K, Gagoski BA, Polimeni JR, Witzel T, Wedeen VJ, Wald LL. Blipped-controlled aliasing in parallel imaging for simultaneous multislice echo planar imaging with reduced g-factor penalty. *Magn Reson Med* 67: 1210–1224, 2012. doi:10.1002/mrm.23097.

Sheremata SL, Bettencourt KC, Somers DC. Hemispheric asymmetry in visuo-topic posterior parietal cortex emerges with visual short-term memory load. *J Neurosci* 30: 12581–12588, 2010. doi:10.1523/JNEUROSCI.2689-10.2010.

Silver MA, Ress D, Heeger DJ. Topographic maps of visual spatial attention in human parietal cortex. *J Neurophysiol* 94: 1358–1371, 2005. doi:10.1152/jn.01316.2004.

Smittenaar P, Kurth-Nelson Z, Mohammadi S, Weiskopf N, Dolan RJ. Local striatal reward signals can be predicted from corticostriatal connectivity. *Neuroimage* 159: 9–17, 2017. doi:10.1016/j.neuroimage.2017.07.042.

Swisher JD, Halko MA, Merabet LB, McMains SA, Somers DC. Visual topography of human intraparietal sulcus. *J Neurosci* 27: 5326–5337, 2007. doi:10.1523/JNEUROSCI.0991-07.2007.

Szczepanski SM, Konen CS, Kastner S. Mechanisms of spatial attention control in frontal and parietal cortex. *J Neurosci* 30: 148–160, 2010. doi:10.1523/JNEUROSCI.3862-09.2010.

Tavor I, Parker Jones O, Mars RB, Smith SM, Behrens TE, Jbabdi S. Task-free MRI predicts individual differences in brain activity during task performance. *Science* 352: 216–220, 2016. doi:10.1126/science.aad8127.

Tobyne SM, Somers DC, Brissenden JA, Michalka SW, Noyce AL, Osher DE. Prediction of individualized task activation in sensory modality-selective frontal cortex with 'connectome fingerprinting'. *Neuroimage* 183: 173–185, 2018. doi:10.1016/j.neuroimage.2018.08.007.

Todd JJ, Marois R. Capacity limit of visual short-term memory in human posterior parietal cortex. *Nature* 428: 751–754, 2004. doi:10.1038/nature02466.

Van Dijk KRA, Hedden T, Venkataraman A, Evans KC, Lazar SW, Buckner RL. Intrinsic functional connectivity as a tool for human connectomics: theory, properties, and optimization. *J Neurophysiol* 103: 297–321, 2010. doi:10.1152/jn.00783.2009.

Vossel S, Geng JJ, Fink GR. Dorsal and ventral attention systems: distinct neural circuits but collaborative roles. *Neuroscientist* 20: 150–159, 2014. doi:10.1177/1073858413494269.

Wang X, He C, Peelen MV, Zhong S, Gong G, Caramazza A, Bi Y. Domain selectivity in the parahippocampal gyrus is predicted by the same structural connectivity patterns in blind and sighted individuals. *J Neurosci* 37: 4705–4716, 2017. doi:10.1523/JNEUROSCI.3622-16.2017.

Xu Y, Chun MM. Dissociable neural mechanisms supporting visual short-term memory for objects. *Nature* 440: 91–95, 2006. doi:10.1038/nature04262.

Yeo BT, Krienen FM, Sepulcre J, Sabuncu MR, Lashkari D, Hollinshead M, Roffman JL, Smoller JW, Zöllei L, Polimeni JR, Fischl B, Liu H, Buckner RL. The organization of the human cerebral cortex estimated by intrinsic functional connectivity. *J Neurophysiol* 106: 1125–1165, 2011. doi:10.1152/jn.00338.2011.